Indian Journal of Fibre & Textile Research
Vol. 49, March 2024, pp. 83-90
DOI: 10.56042/ijftr.v49i1.6210

Color matching of ink-jet textile printing by inversion of forward characterization models using genetic algorithm

Abbas Hajipour & Ali Shams-Nateri[a]
Department of Textile Engineering, University of Guilan, Rasht, Iran

Received 24 April 2022; revised received and accepted 28 March 2023

In this study, the prediction of CMYK digital values and inversion of forward characterization models have been investigated using a genetic algorithm (GA). First, the forward characterization of the printer is performed and the optimum *n*-values in YNSN and spectral *n*-value models are obtained. The optimum *n*-values are used for the prediction of CMYK digital values, and the effective area coverages are obtained by GA. Then, the effective area coverages are converted in to CMYK digital values. The results show that the forward characterization of the printer by spectral *n*-value is better than others. Also, the best result of CMYK digital values prediction is obtained by GA using spectral *n*-value as the objective function. So, the quality of forward characterization model is one of the important factors in color matching by GA using inversion of the forward characterization models.

Keywords: Color matching, Digital printing, Genetic algorithm, Ink-jet printing, Inverse characterization, Polyster fabric

1 Introduction

One of the most important methods used for introducing desired color and pattern to textile fabric is printing. Several techniques have been used for textile printing, such as flat-bed, roller, rotary screen, and digital inkjet printing[1]. Among these, the inkjet printing technique has attracted attention in recent years. This is due to associated benefits, such as speed, creativity, flexibility, time-saving, cost-saving, dye-saving, water and energy-saving, and higher resolution of pattern as compared to other technologies[2-7]. So, it is expected that the traditional technologies may be replaced by digital printing technology in the near future[8].

One of the main types of printer devices is the halftone device. In a halftone printer, the different intensity levels of each colorant are produced by modulating the size, shape, and frequency of the printed dots. However, there is a complicated relationship between pixel values of input digital image and color parameters of a printed sample[9,10]. The print quality is one of the most important issues that affects the complexity of this relationship. The print quality on textile surfaces is lower than that on paper surfaces. This is due to the surface of the textile being rough in comparison to paper. So, the characterization of inkjet textile printers is a bigger challenge in comparison to the characterization of inkjet paper printers.

There are two methods to characterize the relationship between the input digital values (such as CMYK) and the colorimetric parameters of printed color (CIEXYZ and CIEL*a*b*), namely forward and inverse characterization approaches. In the forward approach, the colorimetric parameters of the printed colors are predicted by input digital values, while in inverse approach, the input digital values are predicted by colorimetric parameters of the printed colors[9-11].

Many models have been suggested to output color prediction of halftone printers, such as Murray-Davies, Neugebauer, and YNSN, and spectral *n*-value models[11-19]. However, the direct analytical inversion of forward models is not possible and hence several other methods were proposed[20]. Deshpande *et al.*[20] evaluated different models of the inverse printer model to obtain the color separation. The YNSN was used for forward characterization of the printing process. Then, the look-up table and the constrained optimization were applied for the inversion characterization of the printer. In another study, Deshpande *et al.*[21] used spot color overprint for characterization of the n-color printing process. In this study, the inverse printer model based on the look-up table was carried out to obtain the color separation. Liu *et al.*[22] performed a color separation algorithm based on the Cellular Yule-Nielsen modified Spectral Neugebauer (CYNSN). In the Cellular Neugebauer

[a]Corresponding author.
E-mail: a_shams@guilan.ac.ir

model, the space is reduced by providing more primaries, for which interpolation is performed[11]. Then, an adaptive cell-search algorithm was proposed to obtain the backward CYNSN model.

In this research, a genetic algorithm (GA) is proposed to obtain inversion of forward characterization models and prediction of CMYK digital values of input digital image. GA is a most powerful tool that can be used for solving optimization problems and for testing and fitting quantitative models. GA is based on the principle of genetics and evolution, and is a parallel optimization algorithm. The GA is a stochastic global search method operating on a population of (typically random) individuals, each representing a possible solution to a given problem spread throughout the search space[23-25]. First, the reflectance spectra of inkjet-printed samples have been obtained by a spectrophotometer, and different models as Neugebauer, YNCN, and spectral n-value are applied for forward characterization of the printer. The YNCN and spectral *n*-value forward model are optimized by changing the *n*-value. Then, the optimum condition is used for inverse characterization and color separation by GA. To investigate the performance of various proposed techniques, the accuracy of CMYK digital values prediction has been estimated using the relative error and MSE.

2 Materials and Methods

2.1 Materials

The plain-woven polyester fabric, purchased from Mahtab baft, Iran, was used. Bemacron Blue P-BG (C.I. Disperse Blue 73), Bemacron Scarlet S-BWFL (C.I. Disperse Red 74), and Bemacron Yellow S-4G (C.I. Disperse Yellow 227) were supplied by Bezema, Switzerland and were used for inks preparation of cyan, magenta and yellow respectively. Ethylene glycol, 2-propanol and acetic acid, supplied by Merck, Germany, and a dispersing agent, supplied by Kohan Taj Kimiya, Iran, were used for ink preparation.

2.2 Ink Formulation

The used disperse water-based inks contained 4% (w/v) disperse dye, 70% (v/v) distilled water, a mixture of 2-propanol/ethylene glycol 20/5 (v/v) as a miscible solvent, and 5% (w/v) dispersing agent. The prepared mixture was homogenized for 10 min using a Sonicator Sonopuls UW 3200 (Bandelin, Germany) at average temperature of 21°C. Then, the homogenized disperse water-based ink was filtered through a 2-µm filter. This filtration process is necessary to remove the insoluble impurities and to prevent clogging of the printer's nozzles[6,26-28]. After the preparation of cyan (blue), magenta (red), and yellow inks, the black (gray) ink was prepared by mixing the same proportion of the three prepared inks.

2.3 Inkjet Printing

The inkjet printing of the polyester fabrics was performed using an Epson L130 inkjet printer. Since, this kind of printer is specifically designed for inkjet printing on paper sheets, some modification of the printing manner is necessary. For the printing of fabric samples, the samples were cut to A5 size and then attached to A4 papers. These polyester samples were printed on as easily as paper.

The IT8.7/4-2005 CMYK target was used for sample preparation and printer characterization which consisted of 1617 samples at various digital values of CMYK. The printed polyester samples were fixed by an SDL Pad-Thermosol at 190°C for 90 seconds. Then, the fixed samples were reduction-cleared using a solution containing 2 g/L sodium dithionite and 1.5 g/L sodium carbonate at 60°C for 20 min with a liquor-goods ratio of 20:1. Finally, the polyester samples were rinsed and dried[28]. Figure 1 shows an image of a printed samples.

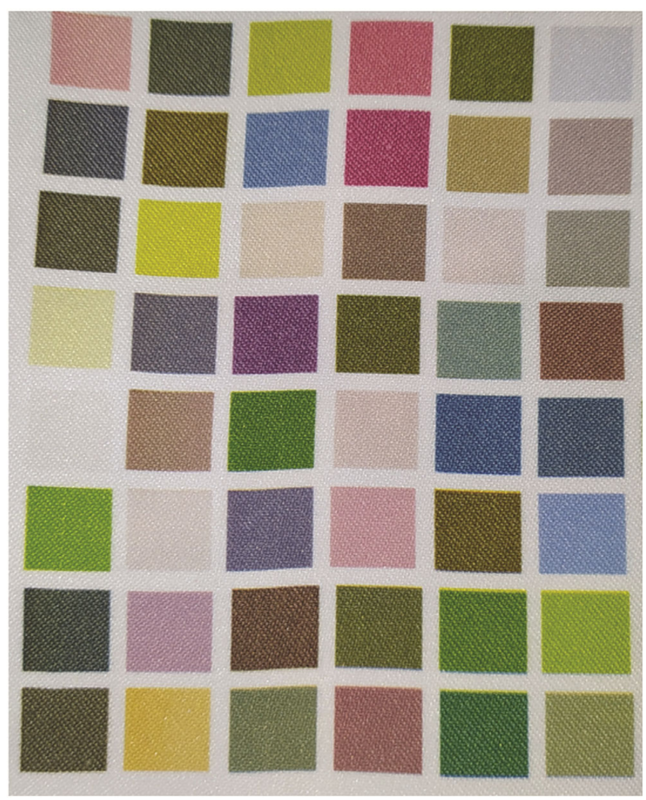

Fig. 1 — An image of a printed sample

2.4 Color Measurements

The reflectance spectra and color parameters of inkjet-printed samples were measured using an i1 Pro 2 spectrophotometer within the visible spectrum at 36 wavelengths with 10 nm intervals from 380 nm to 730 nm over gray background. CIELab coordinates[29-31] (L*, a*, b*, C*, h, where, L* describes the lightness, a* the redness-greenness, b* the yellowness-blueness, C* represents the saturation, and h represents the hue angle) were measured under 10 degrees standard observer and D65 standard illuminant.

2.5 Forward Characterization of Printer

The forward characterization of the printer was performed by Neugebauer, YNCN, and spectral n-value models. The forward characterization using the Neugebauer model was achieved using the following equation:

$$R_{\lambda} = \sum_{i=1}^{2^k} F_i R_{\lambda,i} \qquad \ldots(1)$$

where k is the number of primary inks; F_i, the fractional area coverage of *i*th Neugebauer primary; and $R_{\lambda,i}$, the reflectance spectrum of *i*th Neugebauer primary alone on the surface with 100% area coverage. For a four-color subtractive printing, 16 Neugebauer primaries are needed. The fractional areas occupied by each Neugebauer primary are obtained according to Demichel's equations. Fraction area coverage by each Neugebauer primary is calculated according to Table 1. In this table, c, m, y, and k are effective area coverage of cyan, magenta, yellow and black inks respectively. The reflectance spectra and the color strength (*K*/*S*) of Neugebauer primaries are shown in Fig. 2.

Table 1 — Fraction area coverage by the each primary of the Neugebauer model

Parameter	Ink combination	Reflectance	Fraction of area
F_1	No ink (white)	$R_{\lambda,1}$	$(1-c)(1-m)(1-y)(1-k)$
F_2	C (cyan)	$R_{\lambda,2}$	$c(1-m)(1-y)(1-k)$
F_3	M (magenta)	$R_{\lambda,3}$	$(1-c)m(1-y)(1-k)$
F_4	Y (yellow)	$R_{\lambda,4}$	$(1-c)(1-m)y(1-k)$
F_5	K (black)	$R_{\lambda,5}$	$(1-c)(1-m)(1-y)k$
F_6	CM	$R_{\lambda,6}$	$cm(1-y)(1-k)$
F_7	CY	$R_{\lambda,7}$	$c(1-m)y(1-k)$
F_8	CK	$R_{\lambda,8}$	$c(1-m)(1-y)k$
F_9	MY	$R_{\lambda,9}$	$(1-c)my(1-k)$
F_{10}	MK	$R_{\lambda,10}$	$(1-c)m(1-y)k$
F_{11}	YK	$R_{\lambda,11}$	$(1-c)(1-m)yk$
F_{12}	CMY	$R_{\lambda,12}$	$cmy(1-k)$
F_{13}	CMK	$R_{\lambda,13}$	$cm(1-y)k$
F_{14}	CYK	$R_{\lambda,14}$	$c(1-m)yk$
F_{15}	MYK	$R_{\lambda,15}$	$(1-c)myk$
F_{16}	CMYK	$R_{\lambda,16}$	$cmyk$

One of the most important uses of the Murray-Davies model is to predict the effective area coverage. The reflectance spectra of a halftoned sample using Murray–Davies model can be obtained using the following equation:

$$R_{\lambda} = a_t R_{\lambda,t} + (1-a_t) R_{\lambda,s} \qquad \ldots(2)$$

where R_{λ} is the predicted reflectance spectrum; a_t, the fractional area coverage of the ink; and $R_{\lambda,t}$ and $R_{\lambda,s}$, the reflectance spectrum of ink at full coverage and reflectance spectrum of the bare substrate. In Eq. (2), a_t can be replaced by effective area coverage (a_{eff}) and rearranged as:

$$a_{eff} = R_{meas,adj} R_{t,adj}^{T} (R_{t,adj} R_{t,adj}^{T})^{-1} \qquad \ldots(3)$$

where $R_{meas,adj}=R_{meas}-R_s$, and $R_{t,adj}=R_t-R_s$, and the superscripts T and -1 represent matrix transpose and inverse respectively[9,11,13,16]. The effective area coverage of each ink was calculated using Eq. (3) at 0, 0.2, 0.4, 0.8, and 1 nominal coverages. The effective area coverage of other nominal coverages was measured using the cubic interpolation method.

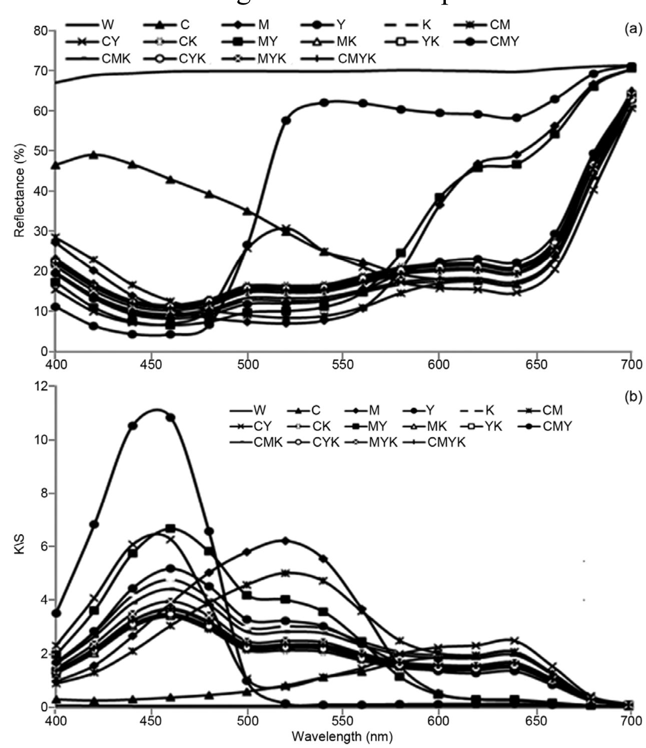

Fig. 2 — (a) Reflectance spectra and (b) color strength (*K*/*S*) of Neugebauer primaries

The forward characterization of a printer using YNSN was achieved using the following equation:

$$R_\lambda = [\sum_{i=1}^{2^k} F_i R_{\lambda,i}^{1/n}]^n \quad \ldots(4)$$

where F_i is exactly same as calculated (Table 1); and n is a scalar parameter which is related to the proportion of paths going through various colorant areas. However, when fitting n-value, effective area coverages must be recalculated and the change of n-value must be noticed in the Demichel equations. So, the effective area coverage is calculated by the Yule-Nielsen model, as shown below:

$$a_{eff} = R_{meas,adj}^{1/n}[R_{t,adj}^{1/n}]^T (R_{t,adj}^{1/n}[R_{t,adj}^{1/n}]^T)^{-1} \quad \ldots(5)$$

Also, in order to improve forward characterization of printer, spectral n-value model is used. Unlike YNSN, in this model n-values are variable with wavelength. So, the required calculation of the spectral n-value model is more than that of YNSN. In this research, in order to reduce calculation, the change of n-value is considered in binary form and changed from 1 to 4 with 0.5 intervals[9,11,13,16]

2.6 Color Matching by Inversion of Forward Models

In this study, inverse characterization of printer using inversion of forward characterization models, such as Neugebauer, YNSN, and spectral n-value models, was performed by GA and the CMYK digital values were predicted. As previously mentioned, 1617 samples of IT8.7/4-2005 CMYK target were used for sample preparation and inverse characterization of printer. To test the proposed model, 100 samples were randomly selected and the other samples were used for optimization of n-value in YNSN and spectral n-values models. The chromaticity distribution of the used samples for forward characterization and inverse characterization of printer as well as Neugebauer primaries in a*-b* axes of CIELAB color space is shown in Fig. 3. In GA method, the CMYK digital values were selected as the parameters (gens) and the fitness function according to Neugebauer, YNSN, or spectral n-value model was applied. The population size and maximum number of generations of used GA were 50 and 100 respectively. In this study, Matlab R2015 a software was used for the GA implementation.

At first, a reflectance spectrum of testing samples was computed by one of the used forward characterization models in each iterations after estimation of effective area coverage. The fitness function based on root mean square (RMS) was calculated by following equation:

$$\text{RMS} = \sqrt{\frac{\sum_\lambda (\Delta R_\lambda)^2}{16}} \quad \ldots(6)$$

where ΔR is the difference between the actual and predicted reflectance spectra. The estimation of effective area coverage would be stopped when the chromosomes (solutions) are converged to the optimal solution and thus the effective area coverage of each

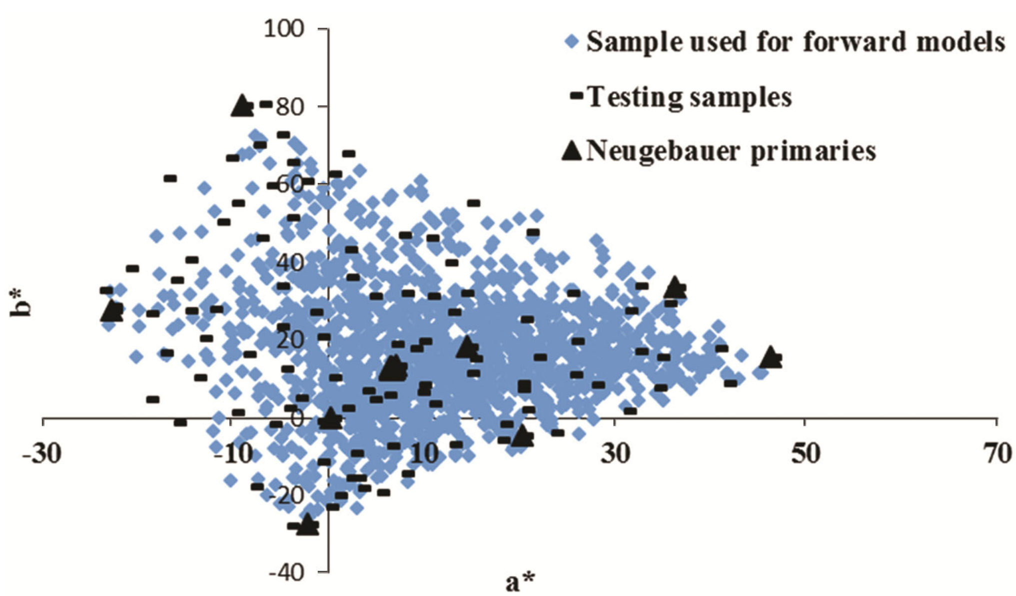

Fig. 3 — Chromaticity distribution of samples used for forward models, testing samples, and the Neugebauer primaries

ink is predicted. Then, the effective area coverages were converted to CMYK digital values by the inverse of the used method in forward characterization. The whole used procedure is schematically shown in Fig. 4.

The accuracy of inverse characterization of the printer was obtained by the relative error between actual (C_a) and predicted (C_p) CMYK digital values were obtained by following equation:

$$E_r = \sqrt{\frac{(C_a - C_p)^2{}_C + (C_a - C_p)^2{}_M + (C_a - C_p)^2{}_Y + (C_a - C_p)^2{}_K}{(C_a)^2_C + (C_a)^2_M + (C_a)^2_Y + (C_a)^2_K}} \quad \ldots(7)$$

3 Results and Discussion

In this research, to find out the optimum *n*-value in YNSN model, the *n*-value has been changed from 1 to 20 with 0.1 intervals and the root mean square (RMS) between predicted reflectance spectra and actual reflectance spectra of 1517 samples used for the optimization of *n*-value is calculated. Also, the derivative of RMS variations of various *n*-values is obtained. The RMS and derivative of RMS of various *n*-values are shown in Fig. 5. The RMS is decreased with an increase of the *n*-value. Also, it can be found that the RMS changes are high at first, but then it decreases with increasing n-value. The derivative of RMS shows that the derivative at 10.3 and higher *n*-values is equal to 0.0000. Therefore, 10.2 has been chosen as the optimum *n*-value in YNSN model.

Also, to obtain optimum *n*-values in spectral *n*-value, the *n*-values are changed in binary form from 1 to 4 with 0.5 intervals and the n-values with the lowest RMS are selected as optimum n-values. The RMS and color difference as an Euclidean distance between the actual and the predicted data by Neugebauer, YNSN, and spectral n-value models with optimum n-values under D65 illuminants and 10º standard observer are obtained and shown in Table 2. As shown in Table 2, the mean of RMS and color difference of Neugebauer are 0.0351 and 7.57 respectively. The mean of RMS and color difference of YNSN are 0.0291 and 6.82 respectively. Also, the mean of RMS and color difference of spectral n-value are 0.0274 and 5.67 respectively. So, the best forward characterization of the printer is made by spectral n-value.

Table 2 — RMS and color difference between the actual and the predicted data by various used forward models

Model	RMS				Color difference			
	Mean	Median	Max	SD	Mean	Median	Max	SD
Neugebauer	0.0351	0.0342	0.1003	0.0144	7.57	6.95	23.48	4.28
YNSN	0.0291	0.0280	0.1003	0.0129	6.82	6.29	22.13	3.56
Spectral n-value	0.0274	0.0262	0.1016	0.0123	5.67	4.90	21.21	3.64

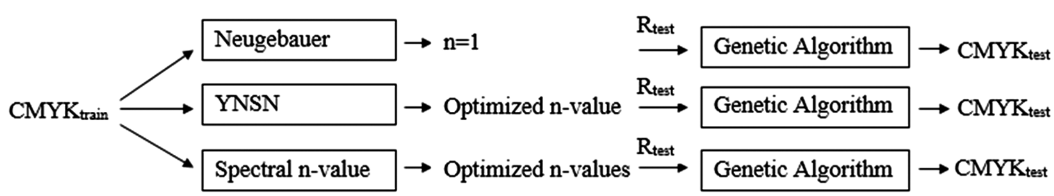

Fig. 4 — Schematic of used methods for prediction of CMYK digital values

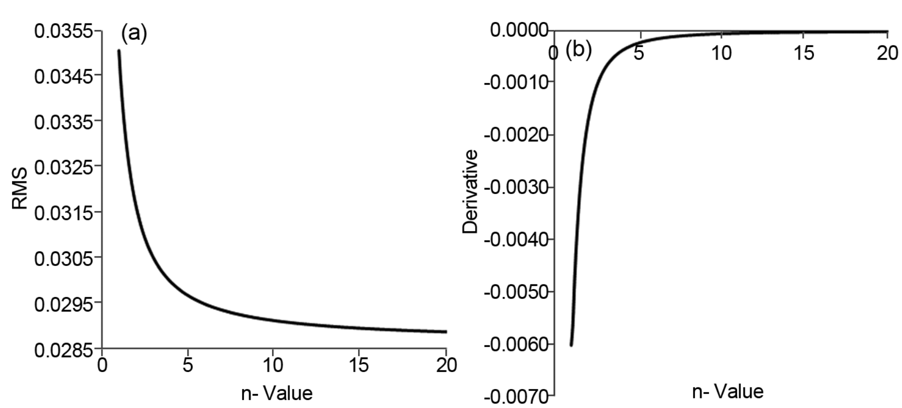

Fig. 5 — (a) RMS and (b) derivative of RMS variations of various *n*-values by YNSN model

Table 3 — Effective area coverage of CMYK in used models

Parameter	Nominal area coverage	Effective area coverage		
		Neugebauer	YNSN	Spectral n-value
C	0.200	0.347	0.239	0.261
	0.400	0.519	0.390	0.435
	0.600	0.811	0.705	0.743
	0.800	0.964	0.913	0.916
M	0.200	0.415	0.256	0.288
	0.400	0.673	0.490	0.533
	0.600	0.909	0.842	0.803
	0.800	0.945	0.898	0.873
Y	0.200	0.370	0.194	0.257
	0.400	0.597	0.367	0.463
	0.600	0.788	0.577	0.674
	0.800	0.893	0.746	0.818
K	0.200	0.445	0.299	0.324
	0.400	0.720	0.577	0.592
	0.600	0.881	0.800	0.798
	0.800	0.977	0.972	0.946

The two most important parameters which changed by optimization of n-value are effective area coverage and reflectance spectra of primaries that are effective in improving prediction. The effective area coverage of CMYK in various used models is shown in Table 3. The effective and nominal area coverages are equal at 0 and 1. It is more than the nominal area coverage in all models. The estimation of effective area coverage by Neugebauer is more than the other models and the obtained values by YNSN are lower than the spectral n-value. However, the effective area coverages of M and K at 0.600 and 0.800 are more than the spectral n-value. The primaries reflectance spectra of the YNSN and spectral n-value are shown in Fig. 6. According to Figs 2 and 6, the shapes of reflectance spectra of the Neugebauer primaries and the YNSN primaries are equal but the reflectance spectra of Neugebauer primaries are more than the reflectance spectra of YNSN primaries. However, the reflectance spectra of spectral n-value primaries are completely different and also lower than the reflectance spectra of Neugebauer primaries.

As previously mentioned, the GA method was used for inversion of the forward models and prediction of the CMYK digital values. The GA fitted the reflectance spectrum of a testing sample by a method of Neugebauer, YNSN, or spectral *n*-value, and the effective area coverage of CMYK is predicted. Then, the effective area coverages of CMYK are converted

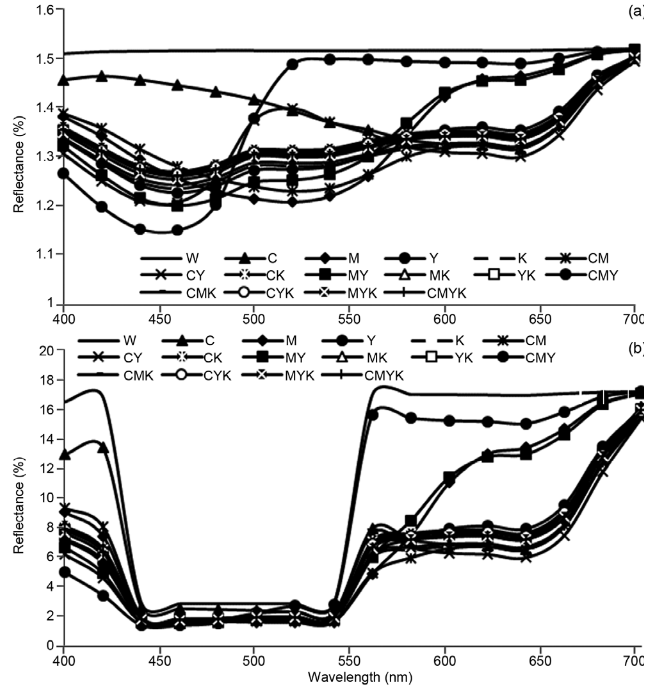

Fig. 6 — Reflectance spectra of (a) YNSN primaries and (b) spectral n-value primaries

to CMYK digital values by the cubic interpolation method. The accuracy of CMYK digital value prediction by GA method with various objective functions, such as Neugebauer, YNSN, or spectral *n*-value, is shown in Table 4. This table indicates that the best result of CMYK digital values prediction is obtained by a GA with spectral *n*-value as the objective function. In this case, the mean, median, max, and SD of relative error are 0.2808, 0.1668, 1.3149 and 0.2937 respectively. Also, the MSE between predicted and actual CMYK digital values is 0.0365. The worst estimation of CMYK digital values is obtained by GA with Neugebauer objective function which the mean, median, max, and SD of relative error of this method are 0.3152, 0.1806, 1.5876 and 0.3325 respectively. The MSE of this method is 0.0424.

The effect of various used methods as GA objective function on fitness function value (RMS) at optimal solution is investigated. The fitness function value at optimal solution of different objective functions is shown in Table 5. It can be seen that the fitness function value at optimal solution of GA with YNSN as the objective function is the best and the RMS between actual and predicted reflectance is lower than others. In this case, the mean, median, max and SD of RMS are 0.0154, 0.0134, 0.0489 and 0.0097 respectively. The worse fitness function value

Table 4 — Accuracy of CMYK digital values prediction by the GA method

Objective function	Relative error					
	Mean	Median	Max	Min	SD	MSE
Neugebauer	0.3152	0.1806	1.5876	0.0001	0.3325	0.0424
YNSN	0.2886	0.1770	2.0220	0.0003	0.3138	0.0395
Spectral n-value	0.2808	0.1668	1.3149	0.0001	0.2937	0.0365

Table 5 — Fitness function value at optimal solution of the GA with various objective functions

Objective function	Mean	Median	Max	Min	SD
Neugebauer	0.0204	0.0191	0.0475	0.0000	0.0101
YNSN	0.0154	0.0134	0.0489	0.0000	0.0097
Spectral n-value	0.0166	0.0156	0.0489	0.0000	0.0095

at optimal solution is obtained by Neugebauer as an objective function which is the mean. Median, max, and SD of RMS are 0.204, 0.0191, 0.0475 and 0.0101 respectively. So, it can be found that although the fitness function value of YNSN at optimal solution is better than others, the obtained effective area coverages are far from actual values. Another important factor is probably the conversion of the effective area coverages to the CMYK digital values.

4 Conclusion

The findings show that the characterization of printing process by spectral n-value is more accurate than other models. The RMS and color difference of YNSN method is 17.1% and 9.9% lower than that of RMS and color difference of Neugebauer respectively, and the RMS and color difference of spectral *n*-value method is 21.9% and 25.1% lower than that of RMS and color difference of Neugebauer respectively. Also, the RMS and color difference of YNSN method is 17.1% and 9.9% lower than that of RMS and color difference of Neugebauer respectively. The prediction of CMYK digital values by GA using the spectral *n*-value as the objective function is better than others. The worst result of CMYK digital values prediction is obtained by the Neugebauer as the objective function. Therefore, improving the forward characterization of the printer improves the color matching. However, the fitness function value at the optimal solution of GA using YNSN as the objective function is better than those of others. It means that the obtained effective area coverages of GA using YNSN as an objective function than the obtained effective area coverages of GA using spectral *n*-value as an objective function are far from actual values.

References

1 Miles L W, *Textile Printing* (Society of Dyers and Colorists, West Yorkshire), 2003.
2 Aldib M , *Color Technol*, 131 (2015) 172.
3 El-Hennawi H M, Shahin A A, Rekaby M & Ragheb A A, *Carbohydr Polym*, 118 (2015) 235.
4 Ataeefard M, *Fibers Polym*, 17 (2016) 1055.
5 Liu Z, Fang K, Gao H, Liu X & Zhang J, *Color Technol*, 132 (2016) 407.
6 Hajipour A & Shams-Nateri A, *Fibers Polym*, 18 (2017) 2462.
7 Mikuž M, Turk S S & Tavčer P F, *Color Technol*, 126 (2010) 249.
8 Gorgani A S & Shakib N, *Color Technol*, 129 (2013) 109.
9 Sharma G, *Digital Color Imaging Handbook* (CRC Press LLC, New York), 2003.
10 Zhao L & Chen G, *Comput Model New Technol*, 18 (2014) 133.
11 Wyble D R & Berns R S, *Color Res Appl*, 25 (2000) 4.
12 Xi S & Zhang Y, *Optik*, 124 (2013) 2103.
13 Hébert M & Hersch R D, *Color Res Appl*, 40 (2015) 383.
14 Ke N, He X, Wang Y & Zhang Y, *Optik*, 125 (2014) 6242.
15 Deshpande K & Green P, *A simplified method of predicting the colorimetry of spot color overprints*, paper presented at 18th Color and Imaging Conference, Texas (USA) 2010, p 213-216.
16 Mestha L K & Dianat S A, *Control of Color Imaging Systems: Analysis and Design* (CRC Press LLC, Boca Raton), 2009.
17 Qu Y & Gooran S, *J Imag Sci Technol*, 56 (2012) 10506-1.
18 Garg N, Singla A & Hersch R, *J Imag Sci Technol*, 52 (2008) 40908-1.
19 Hersch R D, Emmel P, Collaud F & Crété F, *J Electron Imag*, 14 (2005) 033001-1.
20 Deshpande K, Green P & Pointer M R, *Colour separation of n-colour printing process using inverse printer models*, paper presented at 22nd Color and Imaging Conference, Massachusetts (USA) 2014, p 194-199.
21 Deshpande K, Green P & Pointer M R, *Opt Express*, 22 (2014) 31786.
22 Liu S, Tian Q, Zhu M & Liu Z, Spectral Image Color Separation Algorithm Based on Cellular Yule-Nielson Spectral Neugebauer Model, edited by Zhao P, Ouyang Y, Xu M, Yang L & Ren Y, *Applied Sciences in Graphic Communication and Packaging* (Springer, Singapore), 2018, 47-53.
23 Mitchell M, *An Introduction to Genetic Algorithms*, (MIT Press, London), 1998.
24 Chambers L D, *Practical Handbook of Genetic Algorithms: Complex Coding Systems* (CRC press LLC, Boca Raton), 1999.
25 Shams-Nateri A, Hasanlou E & Hajipour A, *Pigment Resin Technol*, 18 (2018) 20.

26 Karanikas V, Nikolaidis N & Tsatsaroni E, *Text Res J*, 83 (2013) 450.
27 Karanikas E, Nikolaidis N & Tsatsaroni E, *Fiber Polym*, 17 (2016) 248.
28 Karanikas E, Nikolaidis N & Tsatsaroni E, *Prog Org Coat*, 76 (2013) 1112.
29 Lee H C. Introduction to *Color Imaging Science* (Cambridge University Press Cambridge), 2005.
30 Kuehni R G , Color: *An Introduction to Practice and Principles* (Wiley, Hoboken), 2012.
31 Schanda J, *Colorimetry*: *Understanding the CIE System* (Wiley, Hobokon), 2007.